Molecular Biology of the Cell
Vol. 14, 417–431, February 2003

Convergence of Non-clathrin- and Clathrin-derived Endosomes Involves Arf6 Inactivation and Changes in Phosphoinositides

Naava Naslavsky, Roberto Weigert, and Julie G. Donaldson*

Laboratory of Cell Biology, NHLBI, National Institutes of Health, Bethesda, Maryland 20892

Submitted April 11, 2002; Revised July 24, 2002; Accepted October 25, 2002
Monitoring Editor: Keith Mostov

The trafficking of two plasma membrane (PM) proteins that lack clathrin internalization sequences, major histocompatibility complex class I (MHCI), and interleukin 2 receptor α subunit (Tac) was compared with that of PM proteins internalized via clathrin. MHCI and Tac were internalized into endosomes that were distinct from those containing clathrin cargo. At later times, a fraction of these internalized membranes were observed in Arf6-associated, tubular recycling endosomes whereas another fraction acquired early endosomal autoantigen 1 (EEA1) before fusion with the "classical" early endosomes containing the clathrin-dependent cargo, LDL. After convergence, cargo molecules from both pathways eventually arrived, in a Rab7-dependent manner, at late endosomes and were degraded. Expression of a constitutively active mutant of Arf6, Q67L, caused MHCI and Tac to accumulate in enlarged PIP_2-enriched vacuoles, devoid of EEA1 and inhibited their fusion with clathrin cargo-containing endosomes and hence blocked degradation. By contrast, trafficking and degradation of clathrin-cargo was not affected. A similar block in transport of MHCI and Tac was reversibly induced by a PI3-kinase inhibitor, implying that inactivation of Arf6 and acquisition of PI3P are required for convergence of endosomes arising from these two pathways.

INTRODUCTION

Cells internalize plasma membrane and extracellular fluid through a variety of processes that include clathrin-dependent and -independent endocytosis. Clathrin-dependent endocytosis is by far the best understood mechanism. Receptors and other plasma membrane (PM) proteins containing cytoplasmic tyrosine or dileucine motifs are recognized by the adaptor protein 2 (AP2) complex and directed into clathrin-coated pits where they are efficiently internalized (Kirchhausen, 1999). By contrast, little is known about the roles and regulation of other forms of membrane internalization (for reviews, see Dautry-Varsat, 2001 and Nichols and Lippincott-Schwartz, 2001). In particular, the fate and itinerary of membrane proteins and lipids that enter cells through nonclathrin pathways remain poorly understood.

Interest in these pathways has increased because of their involvement in important physiological processes, such as uptake of various toxins (Sandvig and van Deurs, 1990), fluid uptake for antigen sampling in dendritic cells (Garrett *et al.*, 2000; West *et al.*, 2000), and macropinocytosis during stimulation of receptors that induces ruffling (Hewlett *et al.*, 1994; Amyere *et al.*, 2000). Although internalization of cholesterol and sphingolipid-enriched, raft-like domains has been the focus of increased attention (for review see Dautry-Varsat, 2001; Nichols and Lippincott-Schwartz, 2001), fluid and membrane internalization via pinocytosis, macropinocytosis, and phagocytosis represent another large component of clathrin-independent endocytosis. Although pinocytosis is generally assumed to be a constitutive process, macropinocytosis and phagocytosis represent stimulated pathways, dependent on actin-mediated ruffling and a particle stimulus, respectively. The relationship between all of these clathrin-independent pathways has yet to be clearly defined. Although it has been observed that fluid taken up into cells independently of clathrin can reach endosomes containing the transferrin receptor (Hansen *et al.*, 1993), the mechanism whereby such fluid and the membranes containing it are trafficked within the cell is not clear. Are there mechanisms to recycle membrane back to the PM? Further characterization of these pathways will contribute to an understanding of the complexity of endocytic pathways and whether and how these pathways connect within the cell.

Clathrin-independent pathways have been difficult to study because of the lack of identifiable marker proteins and

Article published online ahead of print. Mol. Biol. Cell 10.1091/mbc.02–04–0053. Article and publication date are at www.molbiolcell.org/cgi/doi/10.1091/mbc.02–04–0053.

* Corresponding author. E-mail address: jdonalds@helix.nih.gov.

regulatory molecules that define these compartments and because of variations among different types of cells. We have been studying a PM-endosomal recycling pathway that contains PM proteins lacking signals for AP2/clathrin mediated endocytosis. Once internalized, these membrane proteins can be recycled back to the PM via recycling endosomes that contain Arf6 (Radhakrishna and Donaldson, 1997; Brown *et al.*, 2001). Among the endogenous proteins that traverse this pathway are the integral membrane proteins major histocompatibility class I (MHCI) and integrins and signaling molecules such as src, rac, and Arf6. In HeLa cells, this membrane recycling system is distinct from transferrin receptor recycling pathway (Radhakrishna and Donaldson, 1997; Brown *et al.*, 2001). This is in contrast to CHO cells where the Arf6 and transferrin pathways partially overlap (D'Souza-Schorey *et al.*, 1998). Thus, HeLa cells provide a convenient model for looking at the fate of integral membrane proteins that enter cells through this clathrin-independent mechanism.

In this study, we provide detailed analysis of the trafficking of molecules that traverse this clathrin-independent pathway. These membrane proteins are internalized in distinct endosomes, independently of clathrin, dynamin, and lipid rafts. After inactivation of Arf6, membrane can either be routed back to the PM via the Arf6 recycling compartment or fuse with the classical early endosomal compartment in a PI3P-dependent manner and be routed toward degradation.

MATERIALS AND METHODS

Cells, Reagents, and Antibodies

HeLa and COS cells were grown in complete media (DME supplemented with 10% FBS, 100 μg/ml streptomycin, and 100 u/ml penicillin) at 37°C with 5% CO_2.

Polyclonal antibodies to ARF6 were as described (Radhakrishna and Donaldson, 1997). Tac (the human alpha subunit of the IL-2 receptor) and Tac-Dileucine (Tac-LL) were detected in immunofluorescence antibody-uptake experiments with the monoclonal 7G7B6 anti-Tac (Rubin *et al.*, 1985) and by the polyclonal anti-Tac (prepared and kindly provided by Dr. M.S. Marks and Dr. Juan Bonifacino, NIH, Bethesda, MD). 7G7 anti-Tac was used also to immunoprecipitate Tac and Tac-LL (biotinylation assay, see below). Hybridoma cells producing monoclonal antibodies against human MHC class I (W6/32) recognizing the heavy and light chains of the native MHC I complex (Neefjes *et al.*, 1990) was kindly provided by Dr. Eric Long (NIAID, Rockville, MD) and was used both in immunofluorescence and immunoprecipitation experiments. The MHCI-encoded heavy chain is a type I membrane protein that requires association with the light chain, β2-microglobulin, for proper assembly and transport to the PM. W6/32 recognizes only this assembled form of MHCI complex. Monoclonal anti-Lamp1 (H4A3) was from Developmental Studies Hybridoma Bank (Iowa City, IA). Mouse anticlathrin heavy chain (X22, Affinity BioReagents, Golden, CO) and mouse anti-EEA1 were from Transduction Laboratories (Lexington, KY)

Plasmids and Transient Transfection

Tac, Tac-LL, and Arf6 wild-type and Q67L constructs were in pXS vector (Radhakrishna and Donaldson, 1997). Tac-LL is a chimera containing the extracellular, lumenal, and transmembrane domains of Tac and the cytoplasmic tail of the mouse CD3 containing DKQTLL (Letourneur and Klausner, 1992). Dynamin-2-GFP (wild-type and K44A) in pEGFP was provided by Dr. M. McNiven. The PH domain from PLCδ fused to GFP in pEGFP-N1 as described (Varnai and Balla, 1998) was provided by Dr. T. Balla (NIH, Bethesda, MD). Rab5 and lgp 120 were cloned into EGFP vector and provided by Dr. R Lodge (NIH). Wild-type GFP-Rab7 and its mutants were provided by Dr. B. van Deurs (University of Copenhagen, Denmark). For transfections, HeLa or COS cells were grown on glass coverslips and transfected using FuGene according to manufacturer's instructions (Roche, Indianapolis, IN). Cotransfections for immunofluorescence and biotin pulse-chase experiments were performed with 1 μg of each plasmid per 35-mm plate. Experiments were carried out 15–24 h after transfection.

Immunofluorescence

Fifteen- to 24 h after transfection, cells on coverslips were fixed with 2% formaldehyde in PBS at room temperature for 10 min and subjected to immunofluorescence staining (Radhakrishna and Donaldson, 1997). Intracellular staining was performed in the presence of 0.2% saponin. All secondary fluorophore-conjugated antibodies were from Molecular Probes (Eugene, OR). Alexa 488 or Alexa 594 goat anti-mouse or goat anti-rabbit were used as secondary antibodies. For triple labeling Alexa 546 goat anti-mouse IgG1 and Alexa 647 goat anti-mouse IgG2a were used to detect W6/32 and anti-EEA1, respectively. Polyclonal anti-Tac was detected with Alexa 488 goat anti-rabbit.

Internalization of Surface Antibody and DiI-LDL

To assess internalization of Tac, Tac-LL, and MHCI, cells were chilled to 4°C and incubated with the corresponding antibody for 30 min in an ice/water bath to label the cell surface. Unbound antibody was rinsed with cold PBS, and cells were incubated in preheated complete media for the indicated internalization time at 37°C. For experiments involving cointernalization of MHCI and DiI-LDL, assays were performed as described above, with 10 μg/ml DiI-LDL added to the internalization time at 37°C. After internalization, antibodies remaining at the cell-surface were then removed (stripped) by a 30-s rinse with 0.5% acetic acid, 0.5 M NaCl, pH 3.0, washed in PBS briefly, and then fixed for 10 min in 2% formaldehyde at RT. Control incubations indicate that this treatment removes nearly all surface-bound antibody. Internalized cargo molecules were visualized using appropriate secondary antibody conjugated to Alexa 488 (green) or Alexa 594 (red) in the presence of 0.2% saponin. Costaining was performed on fixed and permeabilized cells.

Confocal Microscopy and Analysis of Colocalization

Images were obtained using Zeiss 510 LSM confocal microscope (Thornwood, NY) with 63× PlanApo objective. Presentation of figures was accomplished in Adobe Photoshop (San Jose, CA). To quantify the level of colocalization, 8–10 cells per experimental condition were randomly selected on the same coverslip among those that were well spread and showed a well resolved pattern for the anti-MHCI–labeled structures (green channel). To avoid a biased selection, the other two channels (showing EEA1 and LDL) were not evaluated before the acquisition of the images. Levels for the laser power, detector amplification, and optical sections (1 μm), were optimized for each channel before starting the quantification. Images of single cells were acquired at the same magnification, exported in a TIFF format, and processed by Metamorph 4.6 (Universal Imaging Corp., West Chester, PA). The Metamorph Measure Colocalization Function was used to calculate the area of the region of overlap between two fluorescent probes (area overlap) and their total area as well. The area overlap for the anti-MHCI/LDL– and anti-MHCI/EEA1–labeled structures were reported as percentage

of the anti-MHCI total area, whereas that of LDL/EEA1 labeled structures was reported as percentage of the LDL total area.

Measurement of Internalization by Cell ELISA

HeLa cells were plated in 24-well dishes (SonicSeal, Nalgene Nunc International, Rochester, NY) at a concentration of 100,000 cells/well and transfected the next day with different plasmids (0.2 μg DNA/well). Twenty-four hours after transfection cells were cooled and incubated with 150 μl/well of monoclonal anti-human IL-2 receptor (anti-CD25) conjugated to biotin (BioSource International, Camarillo, CA) at a concentration of 1:30 in complete media for 30 min at 4°C. Unbound antibody was rinsed, and cells were switched to 37°C with complete media for 2–15 min and then were immediately fixed in 2% formaldehyde. Fixed cells were incubated with 0.1 μg/ml streptavidin-HRP (prepared in 5% BSA/PBS) at RT for 15 min (200 μl/well) to label the antibody remaining on the surface and then extensively washed with PBS. Colorimetric reaction was performed with TMB substrate kit (Pierce, Rockford, IL) according to manufacturer's instructions, and OD_{450} was measured. Experiments were carried out in duplicates or triplicates, and data are presented here as a percentage of the initial surface-bound antibody.

Analysis of Degradation of Surface Biotinylated Proteins

HeLa cells were plated in 35-mm wells and transfected at subconfluence. Twenty-four hours after transfection, the cells were washed with ice-cold PBS and cooled on ice. In a typical labeling experiment, 0.3 mg biotin (D-biotinoyl-e-amidocapronic acid-*N*-hydroxysuccinimide ester, Boehringer Mannheim, Mannheim, Germany) was freshly dissolved in 15 μl DMSO and diluted with 1 ml complete media to 0.3 mg/ml. Intact cells were surface biotinylated at 4°C for 30 min with 1 ml biotin. Unbound biotin was removed by thorough washing with ice-cold PBS, quenched with 50 mM NH_4Cl for 10 min, and washed again with PBS. Cells were then incubated for the indicated times with complete media at 37°C and then were lysed with 1 ml of cold lysis buffer (25 mM Tris, pH 7.5, 150 mM NaCl, 5 mM EDTA, 0.5% TX-100, and 0.25% Na deoxycholate) containing protease inhibitors. Endogenous MHC I and both Tac and Tac-LL were immunopreciptated with W6/32 and 7G7 anti-Tac, respectively (200–300 μl/sample). The immunoprecipitate was then separated by PAGE and blotted with streptavidin-HRP to assess the portion of the original surface proteins remaining.

RESULTS

A number of plasma membrane proteins lacking AP2-clathrin targeting sequences have been observed in the Arf6 endosomal recycling pathway in Hela cells (Radhakrishna and Donaldson, 1997). In this study, we used MHCI, an endogenous membrane protein devoid of cytoplasmic clathrin targeting sequences, and Tac, the α subunit of the interleukin 2 (IL2) receptor (Leonard *et al.*, 1984), as reporter molecules for this pathway to examine their itinerary in detail. Both proteins show high colocalization with Arf6 at steady state (Radhakrishna and Donaldson, 1997). We compared the intracellular trafficking of MHCI and Tac to that of low-density lipoprotein (LDL) and Tac-LL, a chimera of Tac with the sequence DKQTLL appended to its cytoplasmic tail. Tac-LL was shown to be efficiently internalized via AP2-clathrin–dependent endocytosis, and delivered to lysosomes (Letourneur and Klausner, 1992; Geisler *et al.*, 1998). The use of transfected Tac and Tac-LL allowed us to compare the trafficking of these membrane proteins using the same antibody that recognizes their common extracellular portion. In parallel, monitoring trafficking of MHCI and DiI-LDL-bound LDL receptor allowed us to examine itineraries of endogenous proteins in untransfected cells. Antibody internalization assays were used here to follow the trafficking of MHCI and Tac in cells utilizing a low pH wash to remove surface antibody as described in MATERIALS AND METHODS. Such assays have been used by others to follow trafficking of MHCI (Coscoy and Ganen, 2000) and Tac chimeras. Anti-Tac 7G7 antibody used in this study has been shown to have no effect on the trafficking kinetics of Tac (Marks *et al.*, 1995) or the heterodimeric or trimeric IL2-receptor (Hemar *et al.*, 1995).

Clathrin-independent and -dependent Cargo Are Internalized in Separate Endosomes that Can Later Converge

We first followed the internalization of endogenous MHCI from the PM and compared it to that of DiI-labeled LDL, bound to the endogenous LDL receptor that is internalized in a clathrin-dependent manner. After 5-min uptake, internalized MHCI was distributed in dispersed, punctate structures that did not coincide with the LDL-labeled structures, but after 20 min, some colocalization of the two cargoes was observed in scattered peripheral endosomes as well as in the juxtanuclear region (Figure 1A). A similar pattern was observed in transfected cells expressing Tac. No colocalization was detected initially between Tac antibody- and LDL-containing structures, but after 20 min, partial colocalization was observed. In both instances, at 20 min some internalized MHCI and Tac colocalized with LDL (see Figure 1A inset, arrows), and some MHCI and Tac could be observed in tubular structures emanating from the perinuclear region (Figure 1A, inset). These tubular structures represent the Arf6-associated recycling compartment described previously (Radhakrishna and Donaldson, 1997) and can be observed in roughly half of the cells. Neither LDL nor Tac-LL were associated with this recycling compartment at any time.

To confirm that these MHCI- and Tac-containing early endosomes exist and are distinct from those carrying clathrin cargo, we examined other combinations of cargo taken up into cells for 5 min. After 5-min internalization, neither Tac nor MHCI colocalized with transferrin, and MHCI did not colocalize with Tac-LL (Figure 1B, top row); however, some colocalization among these cargo molecules could be observed after 20 min (unpublished data). Importantly, after 5-min internalization, MHCI and Tac were present in the same endosomes, and similarly, DiI-LDL and transferrin were present in the same structures (Figure 1B, bottom row). Separate entry and later convergence of MHCI and LDL was also observed in HepG2 and MCF7 cells (our unpublished data). Taken together, these observations, made with endogenous cargo molecules and with transfected proteins, demonstrate that the two pathways are separate initially and, at ~20 min, show some convergence.

Tac and the heavy chain of MHCI are type I membrane proteins lacking cytoplasmic adaptor protein 2 (AP2) targeting sequences that facilitate internalization via clathrin-coated pits. Endocytosis via clathrin-coated pits has been

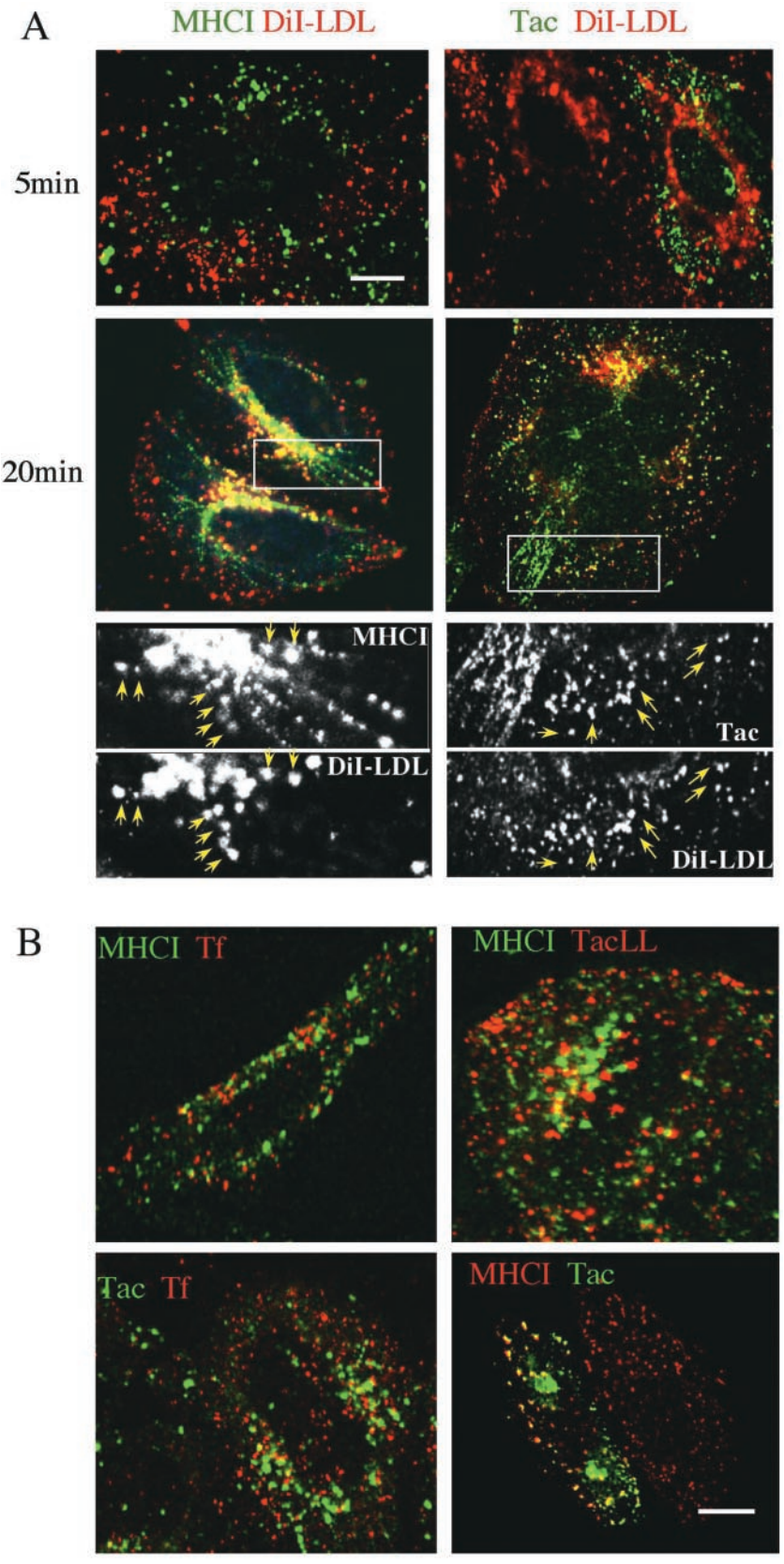

Figure 1. MHCI and Tac enter cells in endosomes distinct from those carrying clathrin-derived cargo and then later merge. (A) Untransfected HeLa cells and those transfected with Tac were allowed to internalize surface-bound anti-MHCI or anti-Tac antibodies, respectively, along with soluble DiI-LDL (10 μg/ml) for 5 and 20 min at 37°C in complete media. Black and white inset at 20 min shows fluorescently labeled structures for each cargo with colocalized structures indicated by yellow arrows. (B) Untransfected and transfected cells expressing either Tac-LL or Tac were allowed to internalize soluble transferrin or DiI-LDL with antibodies to MHCI or Tac for 5 min at 37°C. For both A and B, at the end of the 37°C incubation, surface associated antibodies and DiI-LDL or transferrin were then removed with acid wash, cells were fixed, and internalized antibodies were labeled with fluorescently conjugated secondary antibodies. Bar, 10 μm

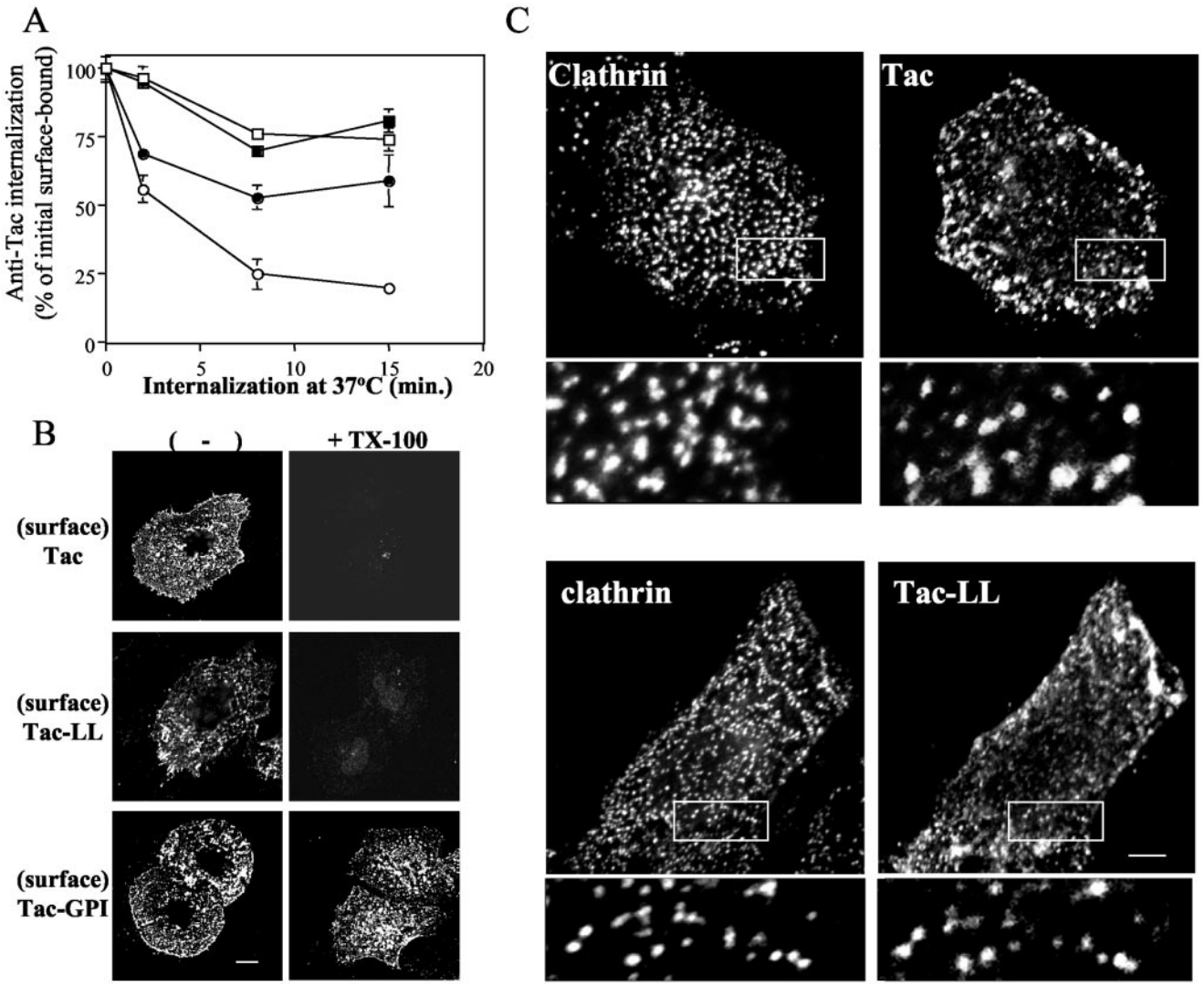

Figure 2. Surface MHCI and Tac are internalized independently of dynamin, are not in rafts, and do not colocalize with clathrin at the PM. (A) HeLa cells were transfected with either Tac (squares) or Tac-LL (circles) and either the wild-type (open symbols) or K44A mutant (filled symbols) of dynamin-2. Tac internalization was monitored by Cell ELISA using biotinylated anti-Tac antibody as described in MATERIALS AND METHODS, and the fraction of Tac antibody remaining on the surface at different time points was recorded. A representative experiment is shown with the mean and SD for triplicates of each time point. (B) HeLa cells were transfected with either Tac, Tac-LL, or Tac-GPI, treated with 1.0% Triton X-100 at 4°C for 3 min, and then fixed. Surface Tac proteins were assessed by incubation with anti-Tac antibodies (without saponin). (C) HeLa cells were transiently transfected with Tac or Tac-LL and fixed. Surface labeling was performed using rabbit anti-Tac antibody in the absence of saponin, followed by a second fixation. Cells were then labeled in the presence of saponin with mouse anticlathrin antibody and with secondary antibodies. Background, surface fluorescence staining was diminished in these images to enhance the punctate pattern of the proteins. Magnified insets are designated. Bar, 10 μm.

shown to depend on the GTPase dynamin, and the expression of the K44A mutant of dynamin-2 inhibits this process (Schmid *et al.*, 1998). To examine whether internalization of Tac was dependent on dynamin, a surface cell ELISA assay was used to quantitatively monitor loss of surface Tac and Tac-LL in cells coexpressing the wild-type or mutant, K44A, dynamin (Figure 2A). In cells expressing wild-type dynamin, the rate of Tac internalization was slower than that of Tac-LL as expected, and the apparent rate of internalization of Tac appeared to diminish between 10 and 15 min (Figure 2A), a time coinciding with appearance of Tac in tubular recycling endosomes (see Figure 1), consistent with recycling back to the PM. The internalization of Tac-LL was inhibited in cells expressing K44A, whereas internalization of Tac was not impaired by expression of either wild-type or K44A mutant of dynamin. The rates of internalization of Tac and Tac-LL in cells coexpressing wild-type dynamin were the same as those in cells expressing Tac or Tac-LL alone

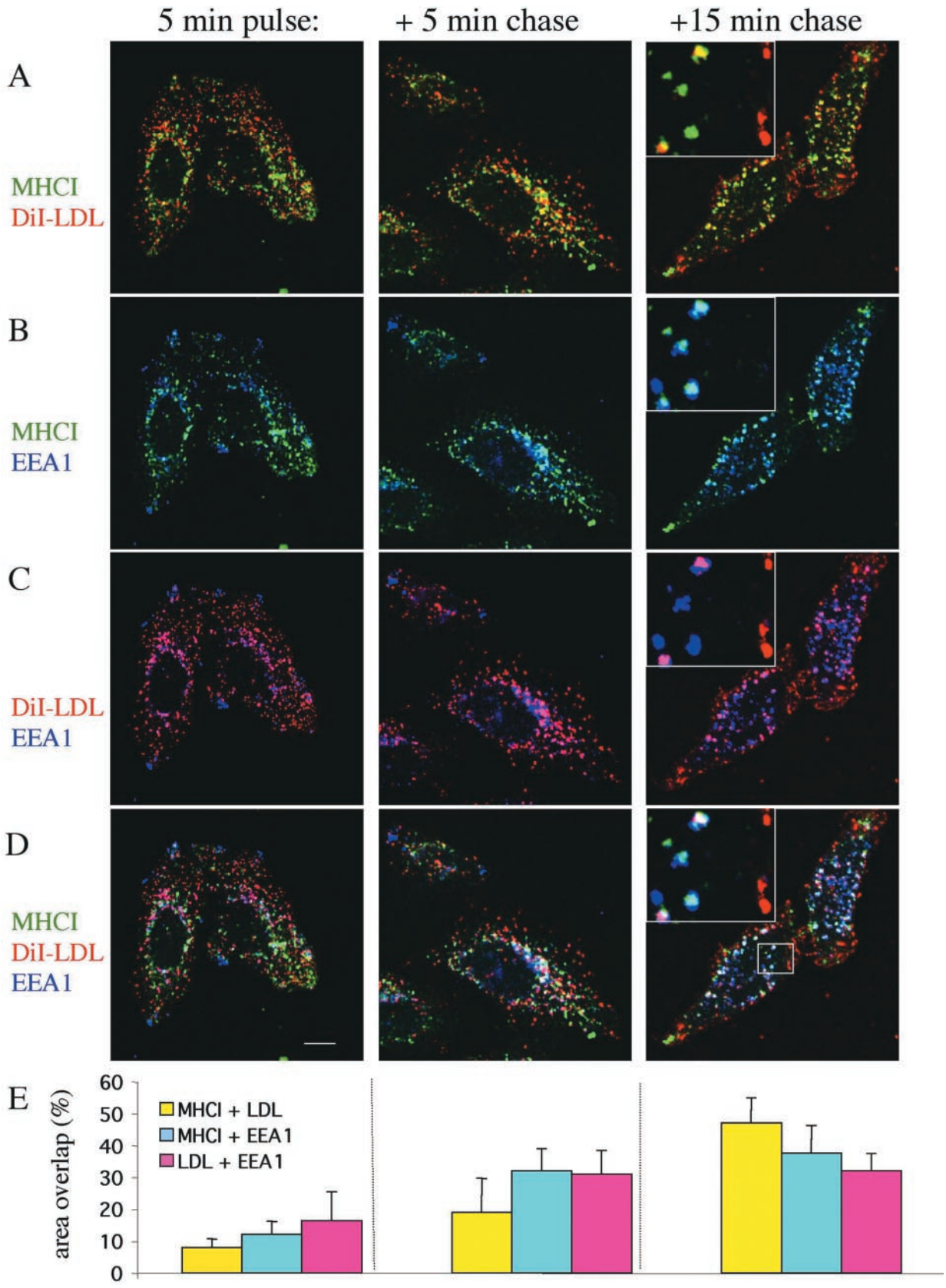
5 min pulse:
+ 5 min chase
+15 min chase
A
MHCI
DiI-LDL
B
MHCI
EEA1
C
DiI-LDL
EEA1
D
MHCI
DiI-LDL
EEA1
E
area overlap (%)
60
50
40
30
20
10
0
MHCI + LDL
MHCI + EEA1
LDL + EEA1

Figure 3.

(unpublished data). All of the above observations were also made in parallel in immunofluorescence experiments (unpublished results). Likewise, the internalization of MHCI, as monitored by immunofluorescence, was unaffected by expression of dynamin K44A (unpublished data). K44A dynamin-2 has also been shown to inhibit caveolae-mediated endocytosis (Dautry-Varsat, 2001). We saw no evidence that Tac was internalized via caveolae or rafts because Tac did not colocalize at the PM with caveolin (unpublished results). Moreover, Tac and Tac-LL, but not Tac with a GPI anchor, were fully solubilized by cold Triton X-100 extraction (Figure 2B), suggesting their lack of enrichment in cholesterol-sphingolipid–enriched microdomains (Brown and Rose, 1992).

We also compared the distribution of surface clathrin with that of surface Tac-LL and Tac molecules by immunofluorescence. Cells that had been transfected with either Tac or Tac-LL were labeled with anti-Tac antibody at 4°C. The cells were then fixed, and clathrin was visualized as described in MATERIALS AND METHODS. Surface Tac distributed in a punctate pattern along the plasma membrane and did not coincide with the more even, punctate fluorescence of clathrin (Figure 2C, compare insets). By contrast, Tac-LL was observed on the surface colocalizing extensively with clathrin (Figure 2C). Although this observation, lack of colocalization of Tac and clathrin at the PM, does not preclude the possibility of Tac actually entering the cell via clathrin-coated pits, taken together with the other data, it suggests that endocytosis of MHCI and Tac occurs through a nonclathrin, non–raft-associated, dynamin-independent mechanism. This pathway may represent the previously observed "bulk" endocytic pathway that persists when dynamin function is inhibited (Damke *et al.*, 1995).

The continuous internalization assays performed in Figure 1A illustrated two distinct endocytic pathways carrying two different cargo-molecules that converge after 20 min of internalization. We sought to better characterize the kinetics of this process and to explore the role of early endosomal autoantigen 1 (EEA1) in the cargo convergence events (Simonsen *et al.*, 1998). For that purpose a pulse-chase immunofluorescence experiment was performed. HeLa cells were allowed to internalize surface bound MHCI antibody and soluble DiI-LDL for 5 min at 37°C, and remaining surface-associated MHCI antibody was immediately removed by low pH rinse (pulse). The cells were then either fixed or incubated in fresh media at 37°C for another 5 or 15 min (chase). After a 5-min pulse, most of the internalized MHCI and DiI-LDL resided in separate endosomal structures (red and green labeling in Figure 3A), similar to that observed in Figure 1A. With further incubation (5 and 15 min) increased colocalization was observed in juxtanuclear structures (yellow spots in Figure 3A).

In this same experiment, we also examined the distribution of EEA1, a protein recruited to early endosomes by phosphatidylinositol 3-phosphate (PI3P) and Rab5 (Simonsen *et al.*, 1998; Lawe *et al.*, 2000). EEA1 facilitates tethering and fusion of early endosomes (Simonsen *et al.*, 1998; McBride *et al.*, 1999); therefore, we wanted to determine whether endosomes containing MHCI have acquired EEA1 before fusion with LDL endosomes. At 5 min, there was little colocalization of MHCI endosomes with EEA1, but this increased especially in the juxtanuclear area after 5 and 15 min chase (see turquoise spots in Figure 3B). Some of these "turquoise spots" observed in Figure 3B appeared white in the triple merge image (Figure 3D), marking postfusion EEA1-associated endosomes, containing both cargoes (Figure 3D, see inset). Yet, other "turquoise spots" remained turquoise in the triple merge (Figure 3D and inset), clearly indicating that a set of MHCI endosomes has acquired EEA1 but not yet fused with LDL-containing endosome. By the 15-min chase, many EEA1-associated MHCI-endosomes also contained LDL and appear white in Figure 3D. Taken together, these data suggest that MHCI-containing endosomes acquire EEA1 before fusion with LDL endosomes.

We quantitated the extent of area overlap between the three fluorophores in this experiment using computer-assisted colocalization analysis as described in MATERIALS AND METHODS. The analysis demonstrates that there is low colocalization between MHCI and LDL at 5 min (8% of MHCI-vesicular area contained LDL),but colocalization increases to 19 and 47% at 5 and 15 min chase, respectively (Figure 3E). At 5-min pulse, both LDL- and MHCI-endosomes had some association with EEA1. For both cargoes, this association increased after 5 and 15 min chase (Figure 3E).

Figure 3 (facing page). MHCI and LDL are internalized in separate endosomes, acquire EEA1, and then fuse. Untransfected HeLa cells were incubated with mouse anti-MHCI at 4°C and then warmed to 37°C in media containing DiI-LDL for 5 min. Surface MHCI antibody was removed by low pH treatment, and the cells were either fixed (pulse) or warmed at 37°C in fresh media for a further 5 and 15 min (chase). Cells were then fixed, and internalized MHCI antibody was visualized with isotype-specific Alexa 546 goat anti-mouse IgG2a. EEA1 was localized with monoclonal anti-EEA1 followed by Alexa 647 goat anti-mouse IgG1. (A) Yellow merged image indicates colocalization between MHCI (green) and DiI-LDL (red). (B) Turquoise merged image indicates colocalization between MHCI (green) and EEA1 (blue) (C) Magenta merged image indicates colocalization between DiI-LDL (red) and EEA1 (blue). (D) White triple-merged image indicates colocalization between all three fluorescent dyes. (E) Quantitative analysis of colocalization as described in MATERIALS AND METHODS. Yellow and turquoise bars indicate percentage of MHCI-area that overlap with LDL and EEA1, respectively. Magenta bar indicates percentage of LDL-area that overlaps with EEA1. The mean and SD are indicated for each condition. Analysis of variance using ANOVA test indicates that the amount of convergence of MHCI and LDL at 5 min was different from that after 5-min chase ($p < 0.05$) and 15-min chase ($p < 0.01$) and that the 5-min chase was different from the 15-min chase ($p < 0.01$).

Changes in Phosphoinositides Accompany Fusion of Clathrin-independent and -dependent Endosomes

Because acquisition of PI3P and recruitment of EEA1 to membranes has been implicated in early endosome fusion and we observe EEA1 associated with MHCI-containing endosomes, we asked whether the activity of a PI3kinase was necessary for MHCI-containing vesicles to fuse with LDL-containing endosomes. Cellular PI 3-kinase activity can be inhibited by treatment of cells with wortmanin or LY294002, the latter a specific and reversible inhibitor (Vlahos *et al.*, 1994). We examined whether LY294002 treatment would inhibit the fusion of vesicles containing cargo molecules coming from the nonclathrin with vesicles containing cargo from clathrin-mediated pathways. To do so, untrans-

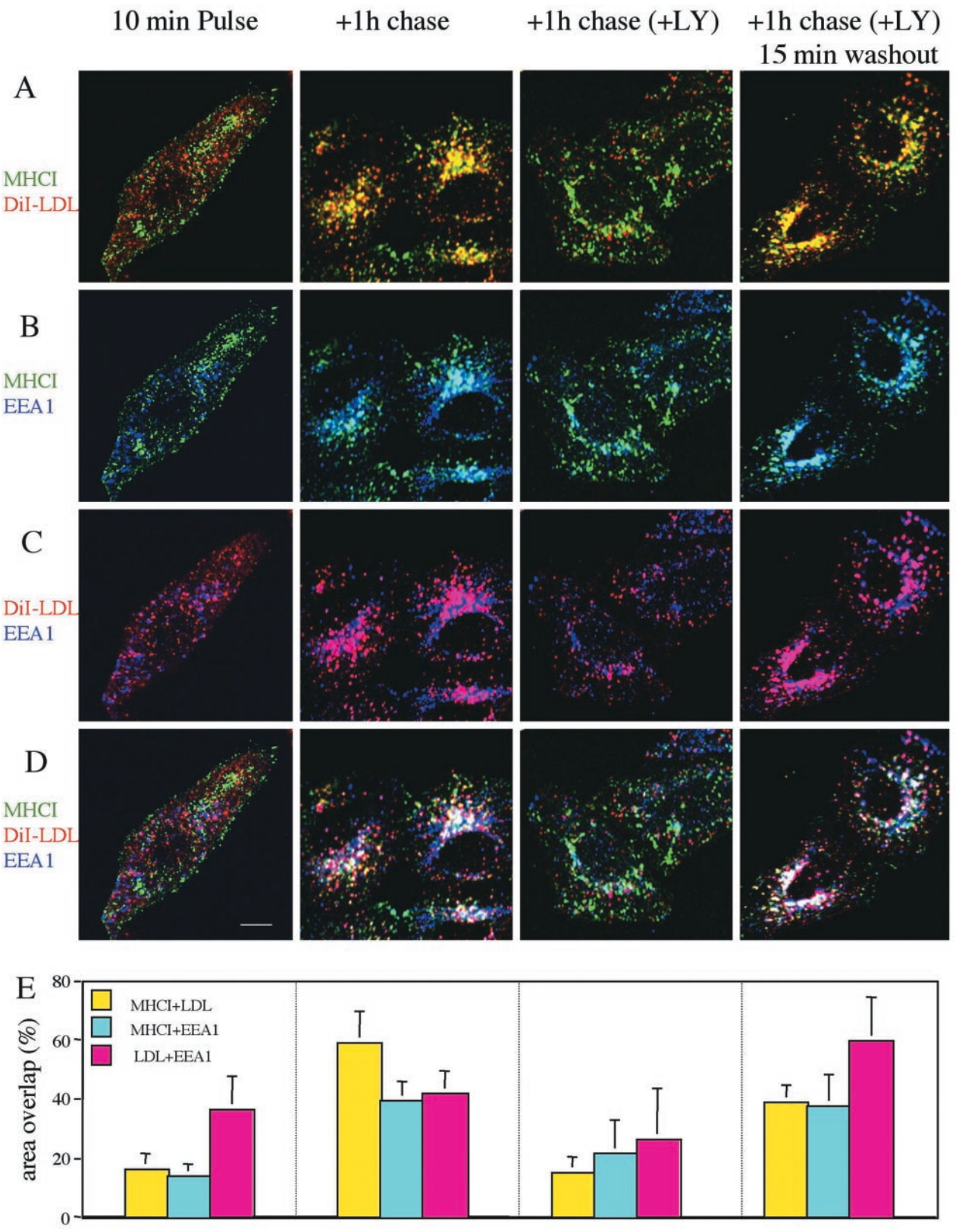
10 min Pulse
+1h chase
+1h chase (+LY)
+1h chase (+LY)
15 min washout
A
MHCI
DiI-LDL
B
MHCI
EEA1
C
DiI-LDL
EEA1
D
MHCI
DiI-LDL
EEA1
E
area overlap (%)
80
60
40
20
0
MHCI+LDL
MHCI+EEA1
LDL+EEA1

Figure 4.

fected HeLa cells were allowed to internalize antibody to MHCI and soluble DiI-LDL for a 10-min pulse. Surface MHCI-antibody and DiI-LDL were then removed with a short acid strip, and cells were chased for another hour with or without LY294002. We opted to preload the cells with cargo in the absence of the drug to avoid any possible effect of LY294002 on the endocytosis rate. Acquisition of EEA1 to both sets of endosomes and their extent of fusion was assessed. Some convergence between MHCI and LDL was detected after the 10-min pulse, but further 1-h incubation in the absence of LY294002 culminated in an extensive overlap between them (Figure 4A). These converged endosomes were clustered near the nucleus and, as expected, also labeled to a large extent with antibody to EEA1 and hence appeared white in the triple merged image (Figure 4D). However, in cells treated with LY294002 during the 1-h chase, MHCI was observed in enlarged endocytic structures that did not colocalize with DiI-LDL-containing endosomes (Figure 4A, LY chase). Both sets of endosomes appeared as separate and scattered, and the lack of fusion between the two was similar to that observed at the 10-min pulse. Nevertheless, both sets of endosomes seemed to be equally sensitive to the drug, as judged by their loss of association with EEA1 in Figure 4E (compare 1-h chase alone and +LY).

Similar observations were made when wortmanin was used in place of LY294002 to inhibit PI 3-kinase (our unpublished results); however, LY294002 is a more specific inhibitor of PI 3-kinase activity and has the advantage of being reversible. Indeed, removal of LY294002 and further incubation for 15 min in the absence of the drug resulted in a massive and nearly complete fusion between the previously separate sets of endosomes containing MHCI and LDL (Figure 4A). Extensive fusion was observable as soon as 5 min after drug removal (unpublished results). The fused endosomes had EEA1 associated with them (appearing white in the triple merge image in Figure 4D). Quantitative analysis of area overlap in this experiment indicated that 16% of MHCI endosomal area contained LDL (yellow) after 10 min (pulse), and this increased to 59% after 1-h chase but was only 15% in the presence of LY294002 (Figure 4E). After removal of the inhibitor, allowing a 15-min recovery, 39% of MHCI endosomal area contained LDL as well.

Figure 4 (facing page). The activity of PI3kinase is necessary for fusion of clathrin-dependent and -independent endosomes. Untransfected cells were labeled with mouse anti-MHCI and DiI-LDL as in Figure 3 and shifted to 37°C for 10 min. Remaining surface MHCI antibody was immediately removed by low pH treatment, and the cells were either fixed (pulse) or warmed at 37°C in fresh media with or without 50 μM LY294002 for 1 h (chase) and fixed. Internalized MHCI antibody was visualized with isotype-specific Alexa 546 goat anti-mouse IgG2a (green). EEA1 was localized with monoclonal anti-EEA1 followed by Alexa 647 goat anti-mouse IgG1 (blue). For washout, after the chase treatment, LY294002 was replaced by fresh media for additional 15 min recovery at 37°C. (A–D) Merged images as in Figure 3. (E) Quantitative analysis of area overlap as in Figure 3. The mean and SD are indicated for each condition. Statistical tests using ANOVA indicate that the amount of convergence of MHCI and LDL after 1-h chase was different from that observed for 1-h chase in the presence of LY ($p < 0.01$) and that the association of EEA1 with MHCI was different at 1-h chase in the absence as compared with the presence of LY ($p < 0.05$). Importantly, upon removal of LY and recovery, there were no significant differences between these values and those obtained for the 1-h chase in the absence of LY.

Degradation of Tac and MHCI Occurs in Late Endosomes/Lysosomes and Requires Rab7

Having demonstrated that a portion of vesicles containing Tac and MHCI fuses with early endosomes containing clathrin cargo, we examined whether these cargo proteins would eventually be delivered to late endosomes and lysosomes and undergo degradation there. The fate of surface MHCI, Tac, and Tac-LL was followed using antibody internalization in the presence of ammonium chloride (NH_4Cl), an inhibitor of lysosomal degradation. Using Rab7 as a marker for late endosomes (Feng *et al.*, 1995; Bucci *et al.*, 2000), we observed that after 7 h of internalization, both Tac and Tac-LL colocalized with wild-type Rab7 (Figure 5A). After 10 h, endogenous MHCI colocalized with lgp120-GFP, a marker for late endosomes/lysosomes, and in cells expressing Tac or Tac-LL, anti-Tac colocalized with Lamp1, another marker for late endosomes/lysosomes (Figure 5B). The use of surface antibodies to follow MHCI and Tac trafficking was not inducing the internalization and delivery of these PM proteins to late endosomes since untransfected cells or cells expressing Tac that were incubated at 37°C in the presence of NH_4Cl for 11 h, showed accumulation of MHCI and Tac respectively, in Lamp1-positive compartments when performing total immunofluorescence staining (our unpublished results).

Degradation of surface Tac, MHCI, and Tac-LL was assessed directly by monitoring the loss of an initial biotinylated pool. Untransfected cells or cells expressing either Tac or Tac-LL were surface biotinylated at 4°C and then incubated at 37°C for 21 h in the absence or presence of NH_4Cl. Cell lysates were immunoprecipitated with antibody to MHCI or Tac and separated by SDS-PAGE, and the blot was probed with HRP-conjugated streptavidin. By 21 h, nearly all of the PM-derived MHCI and Tac were degraded; however, their degradation was inhibited if NH_4Cl was present during the incubation (Figure 5C). We estimate the half lives of Tac, MHCI, and Tac-LL to be between 6 and 8 h. The similarity in half-lives for the surface pool of these proteins indicates that the rate limiting step for degradation is not how rapidly they are cleared from the PM. Inhibition of degradation was also observed using bafilomycin or leupeptin (unpublished results). Because it has been reported that some surface Tac is shed into the media (Marks *et al.*, 1995), we monitored release of biotinylated Tac into the supernatant during the 21 h of chase and found that <5% was shed. As expected, most of the initial surface Tac-LL was degraded after 21 h unless lysosomal degradation was inhibited (Figure 5C).

Trafficking of proteins from early to late endosomes requires Rab7 (Feng *et al.*, 1995; Bucci *et al.*, 2000). Therefore, we examined whether delivery of both cargo molecules to late endosomes was dependent on Rab7 function by following degradation of surface Tac and Tac-LL in cells expressing dominant negative Rab7 T22N. Degradation of surface biotinylated Tac and Tac-LL was inhibited in cells expressing Rab7 T22N (Figure 5D), reflecting the block in trafficking of both cargo molecules to late endosomal compartments. These results imply that degradation of MHCI and Tac is inhibited to the same extent as Tac-LL by Rab7 T22N. Hav-

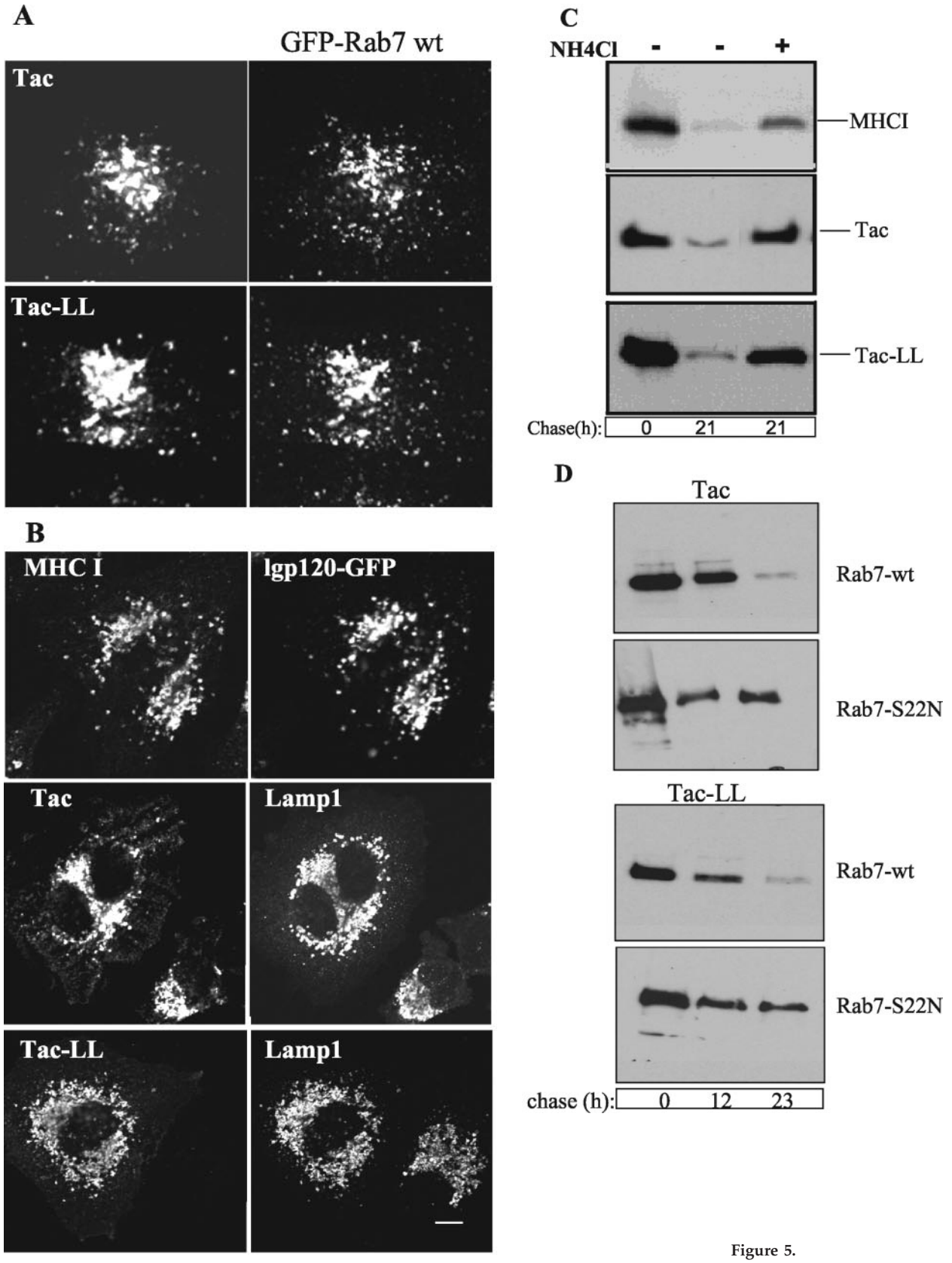
A
GFP-Rab7 wt
Tac
Tac-LL
B
MHC I
lgp120-GFP
Tac
Lamp1
Tac-LL
Lamp1
C
NH4Cl - - +
MHCI
Tac
Tac-LL
Chase(h): 0 21 21
D
Tac
Rab7-wt
Rab7-S22N
Tac-LL
Rab7-wt
Rab7-S22N
chase (h): 0 12 23

Figure 5.

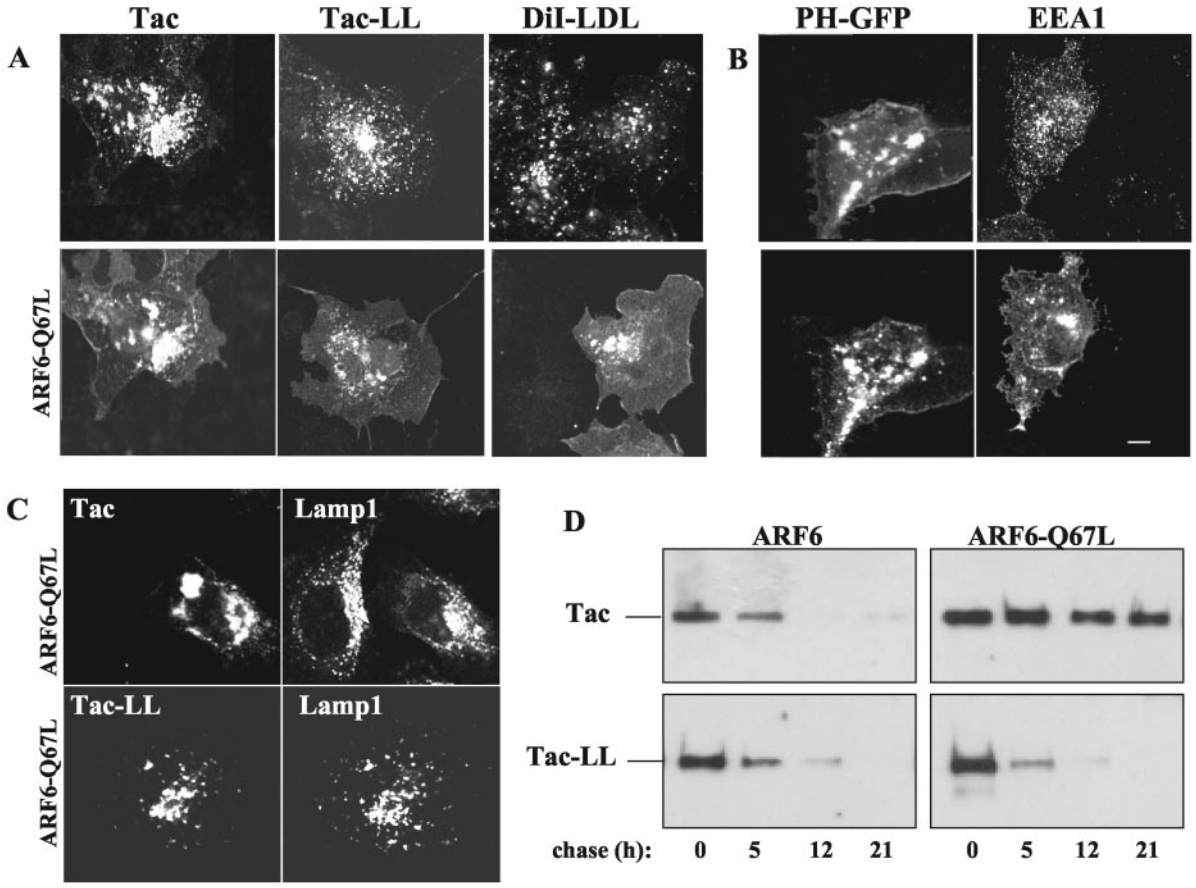

Figure 6. Arf6-Q67L affects trafficking of clathrin-independent cargo but not clathrin-derived cargo. (A) Cos cells were transfected with Arf6 Q67L and Tac (first column), Tac-LL (second column), or Arf6 Q67L alone (third column). Cells were allowed to internalize mouse anti-Tac (first and second column) or DiI-LDL (10 μg/ml; third column) for 1 h at 37°C. (B) Cos cells were cotransfected with Arf6 Q67L and PH-GFP or Q67L alone, and EEA1 was detected in fixed cells using monoclonal anti-EEA1. Cells in A and B were labeled with polyclonal anti-ARF6 followed by the appropriate secondary antibodies. (C) HeLa cells coexpressing Arf6 Q67L and Tac or Tac-LL were incubated with polyclonal anti-Tac antibody for 30 min at 4°C and then incubated for 11 h at 37°C (in the presence of 15 mM NH_4Cl) to allow delivery of PM-bound antibody to lysosomes. After acid wash, cells were fixed, and lysosomes were visualized with monoclonal anti-Lamp1 followed by secondary antibodies. Bar, 10 μm. (D) HeLa cells coexpressing Arf6 wt or Q67L and Tac or Tac-LL were subjected to biotinylation pulse-chase as described in MATERIALS AND METHODS. Lysates were immunoprecipitated with anti-Tac mAb and analyzed as described in Figure 5C.

ing shown in an earlier phase of endocytosis a substantial convergence between cargoes coming from the two different internalization pathways, our interpretation is that the cargo molecules are already in a common structure when arriving at late endosomes/lysosomes.

Arf6 Q67L and Rab5 Q79L Affect Two Distinct Subpopulations of Early Endosomes

To further distinguish the two endocytic pathways and their routes to late endosomes and lysosomes, we sought conditions that would selectively affect trafficking of cargo in the

Figure 5 (facing page). MHCI and Tac get access to late endosomes and lysosomes where they are degraded. (A) HeLa cells cotransfected with GFP-Rab7 and either Tac or Tac-LL were incubated with anti-Tac for 30 min at 4°C. Cells were then incubated at 37°C for 7 h to allow endocytosis of PM-bound antibody to late endosomes. Remaining PM-anti-Tac was removed with acid wash, and cells were fixed. Late endosomes were visualized with GFP-Rab7 and internalized anti-Tac was detected with secondary antibody. (B) Cells transfected with lgp120-GFP, Tac, or Tac-LL were cooled on ice and incubated with anti-MHCI or rabbit anti-Tac for 30 min to label the surface and then incubated at 37°C with complete media containing 15 mM NH_4Cl for 11 h to allow delivery and

Figure 5 (cont). accumulation of antibody to lysosomes. After fixation, lysosomes were visualized with lgp120-GFP (in the case of MHCI) or using mouse anti-Lamp1, followed by the appropriate secondary antibodies. (C) Untransfected cells or cells transfected with either Tac or Tac-LL were surface biotinylated on ice for 30 min and then chased for 21 h with or without 15 mM NH_4Cl in complete media. Lysates were immunoprecipitated with anti-MHCI or anti-Tac antibody and analyzed by SDS-PAGE. Biotinylated proteins were visualized using HRP-conjugated streptavidin. (D) Cells were cotransfected with either Tac or Tac-LL and either wild-type or T22N mutant of Rab7, and after surface biotinylation and internalization, proteins were immunoprecipitated with Tac antibodies as in C above. Bar, 10 μm.

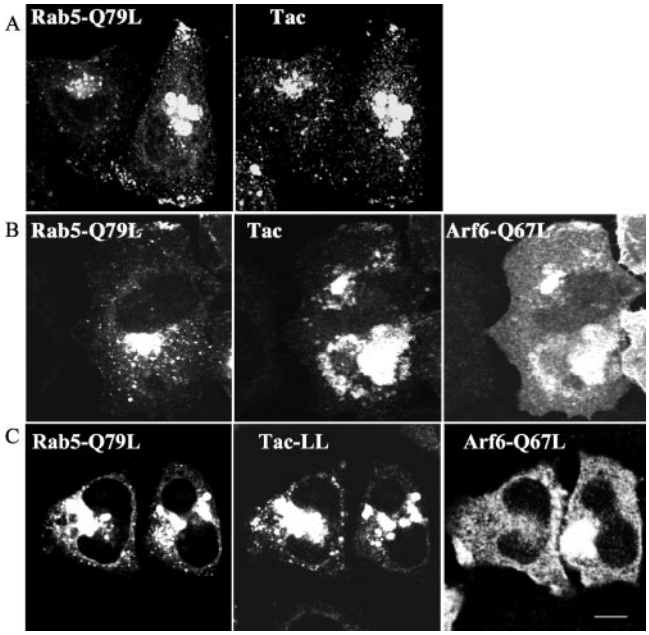

Figure 7. Rab5 and Arf6 affect different internalization pathways. HeLa cells coexpressing GFP-Rab5 Q79L and Tac (A); GFP-Rab5 Q79L, Arf6 Q67L and Tac (B); or GFP-Rab5 Q79L, Arf6 Q67L, and Tac-LL (C) were allowed to internalize monoclonal anti-Tac for 1 h, followed by an acid wash. After fixation, Arf6 was labeled with rabbit anti-Arf6 and Alexa 594 goat anti-rabbit and internalized Tac antibody was detected with Alexa 647 goat anti-mouse. Bar, 10 μm.

Arf6-associated, clathrin-independent pathway. Recently, we reported that expression of constitutively active Arf6 Q67L results in a block of membrane trafficking shortly after endocytosis at short times of expression. These cells accumulate numerous PIP_2-enriched, actin-coated membranes that sequester cargo molecules, which normally traffic through the Arf6 endosomal recycling pathway (Brown *et al.*, 2001). We therefore looked at the effect of this mutant on the trafficking and degradation of Tac and Tac-LL.

The vacuolar structures induced by Arf6 Q67L in HeLa cells accumulate and alter cell morphology, rendering them difficult to image. For this reason, we examined Tac and Tac-LL internalization in COS7 cells that remain flatter upon expression of Arf6 Q67L.

Surface Tac antibody that was internalized for 1 h was sequestered in vacuolar structures that were formed in cells expressing Q67L. By contrast, the distribution of internalized Tac-LL did not coincide with these vacuolar structures nor did DiI-LDL (Figure 6A). The vacuolar structures labeled with a GFP-tagged pleckstrin homology domain of PLCδ (PH) that specifically recognizes PIP_2 (Varnai and Balla, 1998), indicating that the membranes contained PIP_2 (Figure 6B) as previously reported (Brown *et al.*, 2001). Moreover, these PIP_2-enriched membranes were devoid of EEA1 (Figure 6B).

Next, we examined whether Tac and Tac-LL could reach late endosomal/lysosomal compartments in cells expressing Arf6Q67L. After 11 h of antibody internalization to allow optimal loading of lysosomes, Tac was observed in enlarged structures devoid of Lamp1, whereas delivery of Tac-LL to Lamp1-positive compartments still occurred in HeLa cells expressing Q67L (Figure 6C). This impaired delivery of Tac, but not Tac-LL, to degradative compartments was also demonstrated by the biotinylation assay. Expression of wild-type Arf6 had no affect on the degradation rate of either protein, yet expression of Arf6 Q67L specifically inhibited the degradation of Tac, but not that of Tac-LL (Figure 6D). Expression of the dominant-negative mutant of Arf6, T27N, did not affect uptake of Tac nor its trafficking to and degradation in lysosomes (our unpublished results).

Our observations suggest that early endosomes containing Tac or MHCI must undergo inactivation of Arf6 (through GTP hydrolysis) and probably removal or modification of PIP_2 before becoming competent to fuse with the "classical" early-endosome. Having shown evidence that incoming MHCI-vesicles acquire EEA1 (Figure 3B) and fuse with EEA1-endosomes containing LDL (Figure 3A), we sought to demonstrate that MHCI and Tac would also accumulate in enlarged, early endosomes observed in cells that express a constitutively active mutant of Rab5 (Q79L). Rab5 Q79L is believed to cause enlargement of early endosomes through stimulated homotypic fusion (Stenmark *et al.*, 1994). We saw clear localization of Tac within enlarged Rab5 endosomes after 30-min internalization (Figure 7A), and this was also observed, as expected, for Tac-LL (unpublished data). To evaluate the relationship between Arf6 and Rab5, both regulators of early endosomes, we compared the distribution of internalized Tac and Tac-LL in cells coexpressing both Arf6 Q67L and Rab5 Q79L. In the triple-transfected cells we observed Tac trapped in Arf6-induced vacuolar structures but not in enlarged Rab5-endosomes (Figure 7B), whereas Tac-LL accumulated only within enlarged Rab5 endosome (Figure 7C). Thus, sequestration of Tac in Arf6 Q67L vacuoles occurs before fusion with Rab5 early endosomes. These observations provide additional evidence that Tac is internalized primarily through a clathrin-independent pathway, because it cannot reach the enlarged Rab5 endosome once it is sequestered in Arf6 vacuolar structures.

DISCUSSION

In this report, we describe in detail the trafficking of specific trans-membrane proteins that enter cells by a clathrin- and lipid raft–independent mechanism. After internalization, endosomes containing these proteins can either return to the PM in an Arf6-dependent manner or, upon the action of a PI3-kinase and recruitment of EEA1, fuse with the classical early endosome and traffic to late endosomes/lysosomes for degradation (see Figure 8). This clathrin-independent pathway provides the cell with an endocytic membrane-trafficking system that parallels and connects with the "classical" endocytic membrane system and is distinguished by a specific set of GTP-binding proteins, phosphoinositides, and membrane cargo proteins as discussed below.

Integral Membrane Proteins Internalized Independently of Clathrin Can Fuse with "Classical" Early Endosomes

We compared the internalization of two membrane proteins, endogenous MHCI and transfected Tac, that are endocy-

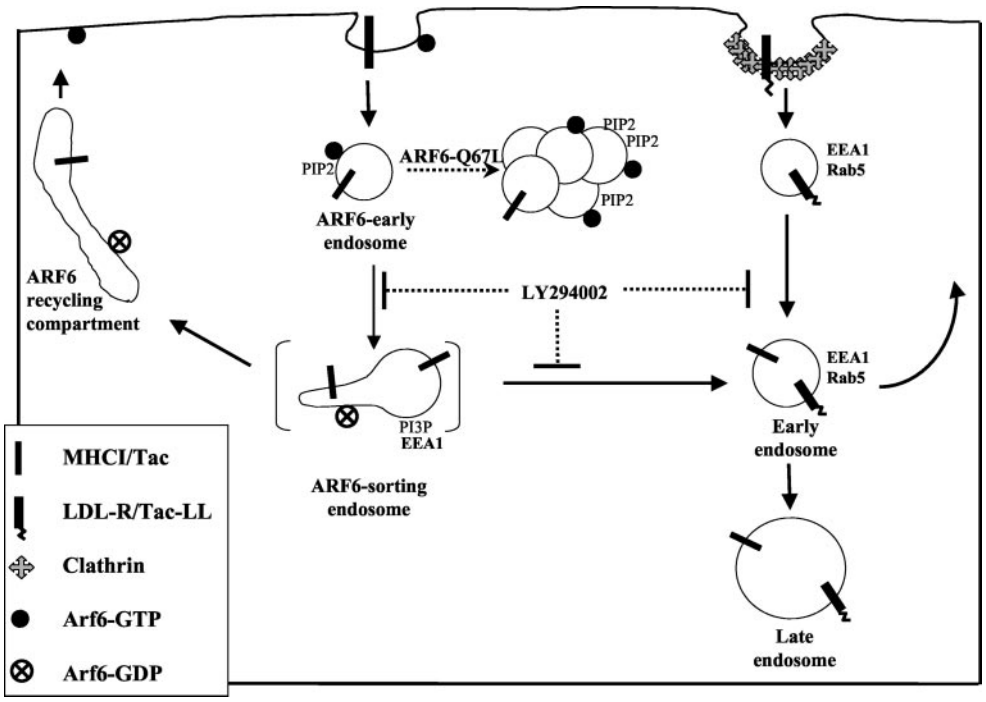

Figure 8. Arf6 inactivation and PI3P synthesis are required for fusion between non–clathrin- and clathrin-derived endosomes. PM proteins (e.g., MHCI, Tac), lacking cytoplasmic clathrin/AP2-targeting sequences enter cells in Arf6-GTP endosomes independent of clathrin-coated pits. These endosomes may undergo homotypic fusion followed by Arf6-GAP stimulated inactivation of Arf6 and loss or modification of PIP_2. In cells expressing Arf6Q67L, inactivation of Arf6 is inhibited, preventing Arf6-derived endosomes from fusing with clathrin-derived endosomes. Instead, extensive homotypic fusion occurs. We speculate that Arf6 endosomes mature or fuse to form a hypothetical Arf6-associated sorting endosome (shown in brackets), where a fraction of the cargo along with Arf6 is recycled back to the PM. Another fraction of the cargo, destined to be degraded, is retained on the membrane that contains the fluid of the endosome. Acquisition of PI3P and recruitment of EEA1 on these endosomes then allows fusion with Rab5/EEA1 early endosomes, thus merging the clathrin-independent and clathrin-derived (LDL-R and Tac-LL) cargo compartments. Inhibition of PI3-kinase with LY294002 (LY) blocks fusion between the two compartments; the exact site of the block and the intermediate that accumulates is not known.

tosed in a clathrin-independent manner, to that of LDL and Tac-LL, proteins that are endocytosed via clathrin-dependent mechanisms. After short periods of internalization, both MHCI and Tac were observed in endocytic structures distinct from those carrying clathrin-dependent cargo. MHCI and Tac were not associated with raft-type membrane domains, and their internalization appeared to be insensitive to inhibition by the K44A mutant of dynamin-2, unlike clathrin-mediated cargo. The distinct mechanism of entry was underscored by the ability of constitutively active Arf6 (Q67L) to trap MHCI and Tac in early Arf6-associated endosomes, which form by stimulated homotypic fusion of Arf6 and PIP_2-associated endosomes (Brown *et al.*, 2001). Clathrin cargo molecules such as LDL and Tac-LL were not sequestered in these structures. Moreover, the trafficking to and degradation of MHCI and Tac in late endosomes/lysosomes was blocked in cells expressing constitutively active Arf6, indicating a requirement for Arf6 inactivation for convergence with the "classical" endocytic pathway. Although inactivation of Arf6 is required for convergence and subsequent routing to lysosomes, Arf6 activation per se, may not be required because the dominant negative Arf6 mutant (T27N) does not appear to block this process. This study represents a significance advance over previous investigations of this clathrin-independent pathway in that we were able to monitor endocytosis of specific membrane proteins into both pathways simultaneously.

Tac chimeras have been used extensively to study the role of cytoplasmic tyrosine and dileucine motifs in trafficking of proteins internalized via clathrin-mediated endocytosis (Marks *et al.*, 1995). In these studies, Marks and colleagues considered Tac to be a control membrane protein that lacked internalization sequences. However, they did observe Tac internalization, albeit at a slower rate than that of a chimera with AP2 sorting sequences (Marks *et al.*, 1995) consistent with our findings (see Figure 2A). The behavior of Tac expressed alone in cells, appears to be distinct from that observed when the two other subunits of the IL2 receptor are also expressed, generating the high-affinity receptor. On ligand binding, the IL2 receptor is internalized by a clathrin-independent mechanism (Subtil *et al.*, 1994), involving dynamin and detergent resistant membrane domains (Lamaze *et al.*, 2001). How the two other subunits alter the internalization route taken by Tac or whether Arf6 affects trafficking of the fully assembled IL2 receptor is not known.

In addition to fusing with early endosomes, fractions of internalized MHCI and Tac are recycled back to the PM via tubular endosomes that are Arf6 positive. These tubular endosomes returning Tac and MHCI, but not LDL, to the PM were observed in Figure 1A and have been observed previously (Radhakrishna and Donaldson, 1997). Furthermore, internalized Tac and MHCI gain access to these tubules between 10 and 20 min and return to the PM, a time that is consistent with the leveling off of the apparent rates of Tac internalization observed between 10 and 15 min (see Figure 2A). Indeed, we recently published data in support of the tubular endosome being a site of MHCI recycling in HeLa cells (Caplan *et al.*, 2002). Furthermore, the Eps15 homology domain containing protein, EHD1, is observed in association with the Arf6 endosome and upon overexpression of EHD1, recycling to the PM of MHCI is enhanced (Caplan *et al.*, 2002). Future studies will quantify the recy-

cling of MHCI and Tac back to the PM in order to compare the amount recycled to that which converges with the clathrin-cargo containing early endosome under various conditions.

Distinct Phosphoinositides and GTPases Define This Pathway

A distinguishing feature of these non–clathrin-derived, early endosomes is that they have associated Arf6 and may initially be PIP_2 enriched. We speculate that these endosomes may undergo a round of homotypic fusion followed by Arf GAP-stimulated inactivation of Arf6 and loss or modification of PIP_2. Synthesis of PI3P occurs on a portion of these endosomes, allowing recruitment of EEA1. Failure to inactivate Arf6, by expression of Arf6 Q67L, leads to stimulated fusion of these PIP_2-associated early endosomes (Brown *et al.*, 2001). Indeed, we observed an accumulation of internalized MHCI (unpublished observations) and Tac in enlarged, PIP_2-positive structures in cells expressing Arf6 Q67L. These structures could not acquire EEA1 (Figure 7C), and hence were unable to fuse with classical early endosomes. Similarly, treatment of cells with LY294002, an inhibitor of PI 3-kinase, blocked formation of PI3P and hence recruitment of EEA1 and therefore prevented their fusion with classical early endosomes (see Figure 4). Although we have yet to identify the PI3-kinase involved, we think it is most likely generating PI3P and not some other 3-phosphorylated phosphoinositide. The requirement for PI3P may be for EEA1 association to allow directed heterotypic fusion between Arf6-derived endosomes and Rab5/EEA1 early endosomes.

Numerous studies in the "classical" endocytic pathway have lead to an appreciation of the role of protein-lipid domains in organizing traffic in the endosomal membrane system (Gruenberg, 2001; Miaczynska and Zerial, 2002). Our studies add an additional component to the early endosomal system explaining how nonclathrin-derived endosomes initially associated with Arf6 and PIP_2 become competent to fuse with the Rab5- and PI3P-associated,classical early endosomes. The identity of the PI 3-kinase isoform involved, as well as the role of Arf6, Rab5, and other Rab proteins in this process will be the subject of further investigations.

The finding that MHCI traffics through this alternative endosomal system has significance for antigen presentation and for understanding the mechanism of downregulation of surface MHCI in viral infections. Our observation of MHCI internalization via a clathrin-independent mechanism is consistent with an earlier study in fibroblasts (Huet *et al.*, 1980). We find that both Tac (Figure 2A) and MHCI (unpublished observations) are internalized into HeLa cells at similar rates (~3%/min) that are close to the rate of 1.7%/min reported in an earlier study for MHCI internalization in B cells (Reid and Watts, 1990). Reid and Watts (1990) also reported that MHCI recycled back to the cell surface, similar to what we find for MHCI and Tac in HeLa cells. There is considerable evidence for peptide loading of exogenous antigens onto MHCI in an acidic endosomal compartment (see Jondal *et al.*, 1996). The pathway we have described here could provide a means for internalized MHCI to reach such an acidic compartment. Finally, the downregulation of MHCI, induced by the HIV protein Nef, is not affected by the K44A mutant of dynamin, whereas the downregulation of CD4, a protein internalized in clathrin-coated vesicles, is inhibited by K44A (Le Gall *et al.*, 2000). This suggests that the downregulation of MHCI involves the clathrin-independent internalization pathway described here.

ACKNOWLEDGMENTS

We thank Tamas Balla, Bo vanDeurs, Robert Lodge, and Mark McNiven for reagents, and Juan Bonifacino, Fraser Brown, Ed Korn, and Jennifer Lippincott-Schwartz for comments on the manuscript.

REFERENCES

Amyere, M., Payraste, B., Krause, U., Van Der Smissen, P., Veithen, A., and Courtoy, P.J. (2000). Constitutive macropinocytosis in oncogene-transformed fibroblasts depend on sequential permanent activation of phosphoinositide 3-kinase and phospholipase C. Mol. Biol. Cell *11*, 3453–3467.

Brown, D., and Rose, J. (1992). Sorting of GPI-anchored proteins to glycolipid-enriched membrane subdomains during transport to the apical cell surface. Cell *68*, 533–544.

Brown, F.D., A.L. Rozelle, A.L., Yin, H.L., Balla, T., and Donaldson, J.G. (2001). Phosphatidylinositol 4,5-biphosphate and Arf6-regulated membrane traffic. J. Cell Biol. *154,* 1007–1017.

Bucci, C., Thomsen, P., Nicoziani, P., McCarthy, J., and van Deurs, B. (2000). Rab7: a key to lysosome biogenesis. Mol. Biol. Cell *11*, 467–480.

Caplan, S., Naslavsky, N., Hartnell, L.M., Lodge, R., Polishchuk, R.S., Donaldson, J.G., and Bonifacino, J.S. (2002). A tubular EHD1-containing compartment involved in the recycling of major histocompatibility complex class I molecules to the plasma membrane. EMBO J. *21*, 2557–2567.

Coscoy, L., and Ganen, D. (2000). Kaposi's sarcoma-associated herpesvirus encodes two proteins that block cell surface display of MHC class I chains by enhancing their endocytosis. Proc. Natl. Acad. Sci. USA *97*, 8051–8056.

D'Souza-Schorey, C., van Donselaar, E., Hsu, V.W., Yang, C., Stahl, P.D., and Peters, P.J. (1998). ARF6 targets recycling vesicles to the plasma membrane: insights from an ultrastructural investigation. J. Cell Biol. *140*, 603–616.

Damke, H., Baba, T., Van der Bliek, A.M., and Schmid, S.L. (1995). Clathrin-independent pinocytosis is induced in cells overexpressing a temperature-sensitive mutant of dynamin. J. Cell Biol. *131*, 69–80.

Dautry-Varsat, A. (2001). Clathrin-independent endocytosis. In: Endocytosis, ed. M. Marsh, Oxford: Oxford University Press, 26–57.

Feng, Y., Press, B., and Wandinger-Ness, A. (1995). Rab 7: an important regulator of late endocytic membrane traffic. J. Cell Biol. *131*, 1435–1452.

Garrett, W., Chen, L., Kroschewski, R., Ebersold, M., Turley, S., Trombetta, S., Galan, J., and Mellman, I. (2000). Developmental control of endocytosis in dendritic cells by Cdc42. Cell *102*, 325–334.

Geisler, C., Dietrich, J., Nielsen, B., Kastrup, J., Lauritsen, J., Odum, N., and Christensen, M. (1998). Leucine-based receptor sorting motifs are dependent on the spacing relative to the plasma membrane. J. Biol. Chem. *273*, 21316–21323.

Gruenberg, J. (2001). The endocytic pathway: a mosaic of domains. Nat. Rev. *2*, 721–730.

Hansen, S.H., Sandvig, K., and van Deurs, B. (1993). Molecules internalized by clathrin-independent endocytosis are delivered to endosomes containing transferrin receptors. J. Cell Biol. *123*, 89–97.

Hemar, A., Subtil, A., Lieb, M., Morelon, E., Hellio, R., and Dautry-Varsat, A. (1995). Endocytosis of interleukin 2 receptors in human T

lymphocytes: distinct intracellular localization and fate of the receptor alpha, beta, and gamma chains. J. Cell Biol. *129*, 55–64.

Hewlett, L.J., Prescott, A.R., and Watts, C. (1994). The coated pit and macropinocytic pathways serve distinct endosomes populations. J. Cell Biol. *124*, 689–703.

Huet, C., Ash, J.F., and Singer, S.J. (1980). The antibody-induced clustering and endocytosis of HLA antigens on cultured human fibroblasts. Cell *21*, 429–438.

Jondal, M., Schirmbeck, R., and Reimann, J. (1996). MHC Class I-restricted CTL responses to exogenous antigens. Immunity *5*, 295–302.

Kirchhausen, T. (1999). Adaptors for clathrin-mediated traffic. Annu. Rev. Cell Biol. *15*, 705–732.

Lamaze, C., Dujeancourt, A., Baba, T., Lo, C., Benmerah, A., and Dautry-Varsat, A. (2001). Interleukin 2 receptors and detergent-resistant membrane domains define a clathrin-independent endocytic pathway. Mol. Cell *7*, 661–671.

Lawe, D.C., Patki, V., Heller-Harrison, R., Lambright, D., and Corvera, S. (2000). The FYVE domain of early endosome antigen 1 is required for both phosphatidylinositol 3-phosphate and Rab5 binding. Critical role of this dual interaction for endosomal localization. J. Biol. Chem. *275*, 3699–3705.

Le Gall, S., Buseyne, F., Trocha, A., Walker, B.D., Heard, J., and Schwartz, O. (2000). Distinct trafficking pathways mediate Nef-induced and clathrin-dependent major histocompatibility complex class I down-regulation. J. Virol. *74*, 9256–9266.

Leonard, W.J. *et al.* (1984). Molecular cloning and expression of cDNAs for the human interleukin-2 receptor. Nature *311*, 626–631.

Letourneur, F., and Klausner, R.D. (1992). A novel di-leucine motif and a tyrosine-based motif independently mediate lysosomal targeting and endocytosis of CD3 chains. Cell *69*, 1143–1157.

Marks, M., Roche, P., van Donselaar, E., Woodruff, L., Peters, P., and Bonifacino, J.S. (1995). A lysosomal targeting signal in the cytoplasmic tail of the beta chain directs HLA-DM to MHC class II compartments. J. Cell Biol. *131*, 351–369.

McBride, H.M., Rybin, V., Murphy, C., Giner, A., Teasdale, R., and Zerial, M. (1999). Oligomeric complexes link Rab5 effectors with NSF and drive membrane fusion via interactions between EEA1 and syntaxin 13. Cell *98*, 377–386.

Miaczynska, M., and Zerial, M. (2002). Mosaic organization of the endocytic pathway. Exp. Cell Res. *272*, 8–14.

Neefjes, J.J., Stollorz, V., Peters, P.J., Geuze, H.J., and Ploegh, H.L. (1990). The biosynthetic pathway of MHC class II but not class I molecules intersects the endocytic route. Cell *61*, 171–183.

Nichols, B.J., and Lippincott-Schwartz, J. (2001). Endocytosis without clathrin coats. Trends Cell Biol. *11*, 406–412.

Radhakrishna, H., and Donaldson, J.G. (1997). ADP-ribosylation factor 6 regulates a novel plasma membrane recycling pathway. J. Cell Biol. *139*, 49–61.

Reid, P.A., and Watts, C. (1990). Cycling of cell-surface MHC glycoproteins through primaquine-sensitive intracellular compartments. Nature *346*, 655–667.

Rubin, L.A., Kurman, C.C., Biddison, W.E., Goldman, N.D., and Nelson, D.L. (1985). A monoclonal antibody 7G7/B6, binds to an epitope on the human interleukin-2 (IL-2) receptor that is distinct from that recognized by IL-2 or anti-Tac. Hybridoma *4*, 91–102.

Sandvig, K., and van Deurs, B. (1990). Selective modulation of the endocytic uptake of ricin and fluid phase markers without alteration in transferrin endocytosis. J. Biol. Chem. *265*, 6382–6388.

Schmid, S.L., McNiven, M.A., and De Camilli, P. (1998). Dynamin and its partners: a progress report. Curr. Opin. Cell Biol. *10*, 504–512.

Simonsen, A. *et al.* (1998). EEA1 links PI(3)K function to Rab5 regulation of endosome fusion. Nature *394*, 494–498.

Stenmark, H., Parton, R.G., Steele-Mortimer, O., Lutcke, A., Gruenberg, J., and Zerial, M. (1994). Inhibition of rab5 GTPase activity stimulates membrane fusion in endocytosis. EMBO J. *13*, 1287–1296.

Subtil, A., Hemar, A., and Dautry-Varsat, A. (1994). Rapid endocytosis of interleukin 2 receptors when clathrin-coated pit endocytosis is inhibited. J. Cell Sci. *107*, 3461–3468.

Varnai, P., and Balla, T. (1998). Visualization of phosphoinositides that bind pleckstrin homology domains: calcium- and agonist-induced dynamic changes and relationship to myo-[^{3}H]inositol-labeled phosphoinositide pools. J. Cell Biol. *143*, 501–510.

Vlahos, C.J., Matter, W.F., Hui, K.Y., and Brown, R.F. (1994). A specific inhibitor of phosphatidylinositol 3-kinase, 2-(4- morpholinyl)-8-phenyl-4H-1-benzopyran-4-one (LY294002). J. Biol. Chem. *269*, 5241–5248.

West, M., Prescott, A., Eskelinen, E., Ridley, A., and Watts, C. (2000). Rac is required for constitutive macropinocytosis by dendritic cells but does not control its downregulation. Curr. Biol. *10*, 839–848.